
Rethinking Graph Out-Of-Distribution Generalization: A Learnable Random Walk Perspective

Henan Sun[†] Xunkai Li[†] Lei Zhu[#] Junyi Han[†] Guang Zeng[#] Rong-Hua Li[†] Guoren Wang[†]

[†] Beijing Institute of Technology

[‡] Jilin University

[#] Ant Group

magneto0617@foxmail.com, cs.xunkai.li@gmail.com, simon.zl@antgroup.com,
hanjy5521@mails.jlu.edu.cn, senhua.zg@antfin.com, lironghuabit@126.com,
wanggrbit@gmail.com

Abstract

Out-Of-Distribution (OOD) generalization has gained increasing attentions for machine learning on graphs, as graph neural networks (GNNs) often exhibit performance degradation under distribution shifts. Existing graph OOD methods tend to follow the basic ideas of invariant risk minimization and structural causal models, interpreting the invariant knowledge across datasets under various distribution shifts as graph topology or graph spectrum. However, these interpretations may be inconsistent with real-world scenarios, as neither invariant topology nor spectrum is assured. In this paper, we advocate the learnable random walk (LRW) perspective as the instantiation of invariant knowledge, and propose LRW-OOD to realize graph OOD generalization learning. Instead of employing fixed probability transition matrix (i.e., degree-normalized adjacency matrix), we parameterize the transition matrix with an LRW-sampler and a path encoder. Furthermore, we propose the kernel density estimation (KDE)-based mutual information (MI) loss to generate random walk sequences that adhere to OOD principles. Extensive experiment demonstrates that our model can effectively enhance graph OOD generalization under various types of distribution shifts and yield a significant accuracy improvement of 3.87% over state-of-the-art graph OOD generalization baselines.

1 Introduction

Graph neural networks (GNNs) have become a fundamental solution of encoder architectures for modeling graph-structured data [30, 38, 3, 20]. They facilitate the efficient computation of node representations, which can be readily adapted to a wide range of graph-based applications, including social network analysis, recommendation systems, anomaly detection and so on [37, 26, 24, 4]. Despite great advances of GNNs, most of existing models follow the i.i.d. assumption, i.e., the testing nodes independently generated from an identical distribution as the training ones [9, 25, 7, 16, 23, 13]. However, this assumption doesn't necessarily conform to the real-world scenarios since numerous spurious correlations among datasets may infect GNNs' training. Recent evidence has demonstrated that GNNs perform unsatisfactorily on Out-Of-Distribution (OOD) data where the distributions of test data exhibit a major shift compared to the training data [1, 11, 5]. Thus, such problem, also known as graph OOD generalization, remains a great challenge to be solved.

Existing graph OOD generalization models for node-level tasks are largely inspired by the concepts from the invariant risk minimization (IRM) and structural causal models (SCMs) [1, 11, 5]. These models employ various mechanisms to extract invariant knowledge shared between the training and testing datasets and discard the spurious correlation among them. Broadly, graph OOD generalization

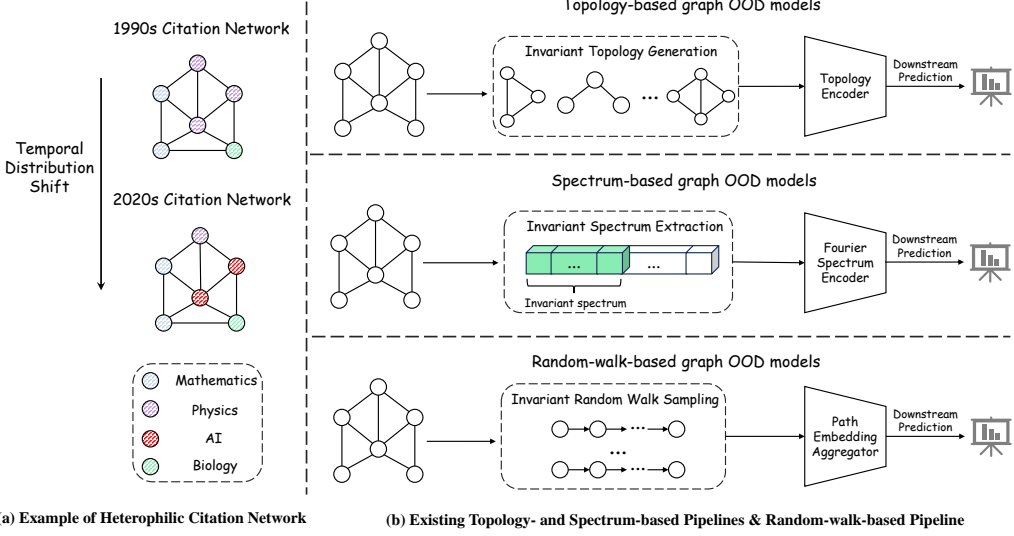


Figure 1: An example of the heterophilic citation network under temporal distribution shift and pipelines of existing graph OOD models. Topology-based and spectrum-based pipelines are the two primary approaches for graph OOD generalization, while the random-walk-based pipeline is the proposed one in this paper.

models can be categorized into two primary approaches: capturing invariant graph topology and capturing invariant graph spectrum, as shown in Figure 1(b) [29, 6, 31, 39, 14, 28, 40]. The first approach interprets invariant knowledge as specific graph topology and leverages techniques such as pseudo-environment-generation to facilitate graph OOD generalization learning. In contrast, models that focus on invariant graph spectrum learning emphasize the acquisition of a stable spectral representation across graphs under multiple environments. These models typically assume that certain spectral components, particularly the low-frequency spectrum, remain invariant. Thus, they introduce perturbations to the remaining spectral components, thereby generating diverse graph data for graph OOD generalization learning. Despite the advancements in the aforementioned methods, they still fail to achieve satisfactory performance in graph OOD generalization learning. Take the heterophilic citation networks of Figure 1(a) as an example, where nodes represent papers and edges denote citation relationships. The objective in such networks is to predict the category of a given paper (e.g., mathematics, physics, AI and biology), and the latent distribution shifts arise due to temporal variations in citation patterns. For instance, in the 1990s, mathematics-related papers were predominantly cited by works in physics and biology, whereas in the 2020s, mathematics-related papers within a similar local topology may exhibit a stronger tendency to be cited by AI-related research. In this scenario, previous graph OOD generalization models exhibit severe limitations as follow:

Limitation 1: The presence of an invariant graph topology across graphs is not assured, as structurally similar topologies may correspond to distinct semantic interpretations under varying distribution shifts. For instance, in the citation network depicted in Figure 1(a), the semantic significance of the local topology formed by nodes around physics papers differs from that of nodes around AI papers, despite the fact that both subgraphs exhibit analogous topological structures.

Limitation 2: The extraction of a universally invariant graph spectrum remains unreliable due to the lack of a well-defined theoretical relationship between the graph spectrum and the formulation of OOD generalization in graphs. For example, in the citation network depicted in Figure 1(a), the graph from the 1990s exhibits stronger homophily, resulting in higher magnitudes in the low-frequency spectrum components and lower magnitudes in the high-frequency components. In contrast, the graph from the 2020s demonstrates increased heterophily, leading to a complete reversal in the distributions across frequency bands. Consequently, no invariant graph spectrum persists in such graphs under temporal distribution shifts.

To address the aforementioned limitations, we utilize learnable random walk sequences as a means of capturing invariant knowledge across graphs under various distribution shifts for node-level tasks. The underlying motivations are derived from two perspectives: **(M1)** Different from the two approaches

illustrated above, learnable random walk sequences are capable of integrating graph topology and node features together into the probability matrix, thus concretizing invariant knowledge into the probability of the next random walk. Intuitively, such learnable-probability-based invariant random walk exists as long as there are invariant knowledge shared across graphs under distribution shifts. **(M2)** Through rigorous mathematical analysis, we demonstrate that learnable random walk sequences exhibit a well-defined theoretical connection to the formulation of graph OOD generalization outlined in Section 3. This approach effectively captures invariant knowledge while mitigating spurious correlations, thereby facilitating robust graph OOD generalization learning. Based on the illustration above, we propose the **Learnable Random Walk** for graph **OOD** generalization model (LRW-OOD). The detailed contributions of this paper are summarized below:

Our contributions. (1) *New Perspective.* To the best of our knowledge, this study is the first to systematically examine the impact of learnable random walk sequences on the graph OOD generalization problems. Our findings offer valuable insights into graph OOD learning, contributing to a deeper understanding of how random walk sequences can enhance model’s performance on datasets under diverse distribution shifts. (2) *New Graph OOD Learning Paradigm.* We propose LRW-OOD, which employs an OOD-aware LRW encoder to adaptively sample sequences that adhere to specific graph OOD principles. This approach enables the model to extract random walk paths that encapsulate sufficient invariant knowledge while effectively eliminating spurious correlations. This novel paradigm offers significant insights into the advancement of graph OOD learning, paving the way for future research in this domain. (3) *SOTA Performance.* We conduct a series of performance evaluations on seven benchmark datasets, comparing our proposed model, LRW-OOD, against nine state-of-the-art graph OOD generalization models. The experimental results demonstrate that the proposed LRW-OOD outperforms the most competitive baselines when utilizing both GCN and GAT as the GNN backbone, achieving an average improvement of 3.87% on graph OOD generalization.

2 Preliminaries

2.1 Problem Formulation

The Semi-supervised Node Classification Tasks on Graphs. We consider a general graph representation method, denoted as $\mathbf{G} = (\mathcal{V}, \mathcal{E})$, where $|\mathcal{V}| = n$ represents the number of nodes and $|\mathcal{E}| = m$ denotes the number of edges. The adjacency matrix (including self-loops) for the graph is $\mathbf{A} \in \mathbb{R}^{n \times n}$, where each entry $\mathbf{A}(u, v) = 1$ if $(u, v) \in \mathcal{E}$ and $\mathbf{A}(u, v) = 0$ otherwise. Additionally, the node feature matrix is represented as $\mathbf{X} = \{x_1, \dots, x_n\}$, where each $x_v \in \mathbb{R}^f$ corresponds to the feature vector associated with node v . The node label is denoted as \mathbf{y} . In the semi-supervised node classification paradigm, the graph is partitioned into a labeled node set \mathcal{V}_L and an unlabeled set \mathcal{V}_U . The classification process leverages the graph topology and the node features, wherein the model is trained using \mathcal{V}_L and subsequently applied to infer the labels of nodes in \mathcal{V}_U .

The OOD Generalizations on Graphs. In this paper, we primarily investigate the problem of graph OOD generalization at the node level, where multiple distribution shifts—such as topology shifts and node feature shifts—occur between the training and testing sets. Formally, this is characterized by a discrepancy in the joint distribution, i.e., $\Pr_{tr}(\mathbf{G}, \mathbf{y}) \neq \Pr_{te}(\mathbf{G}, \mathbf{y})$, where the objective is to accurately predict node labels despite these distribution shifts. The key factors driving such distribution shifts are referred to as confounders or environments, which can be understood through the lenses of data generation distributions and causal inference learning. Since the training and testing sets are derived from distinct environments, spurious confounders may be embedded within the correlations between the graph \mathbf{G} and the label \mathbf{y} . However, despite the presence of these confounding factors, certain invariant or stable properties persist across different environments. The goal of graph OOD generalization models is to learn representations that capture these invariant factors while eliminating the influence of spurious confounders, thereby enhancing model performance under diverse distribution shifts.

2.2 Related works

Graph Neural Networks. GNNs have garnered significant attention due to their efficacy in learning high-quality representations from graph-structured data [9, 25, 36, 35, 10, 33]. While extensive research has been conducted on the expressiveness and representational power of GNNs, their generalization capability remains an open question, particularly in scenarios where the test data is

drawn from distributions different from those of the training data [1, 11, 5]. Following the ideas of invariant risk minimization and structural causal models which reveal that the fundamental challenge of OOD generalization in graph data stems from latent confounder, this paper propose a theoretically grounded model designed to effectively extract the invariant knowledge and discard the spurious correlations across datasets under various distribution.

OOD Generalization Learning on Graphs. The problem of learning under distribution shifts in graph-structured data has increasingly attracted attention within the graph learning research community [29, 6, 31, 39, 14, 28, 40, 27]. SRGNN [39] attempts to address performance degradation by incorporating a regularization term and reducing the disparity between embeddings derived from the training and testing sets. DGNN [6] conducts extensive empirical studies and leverages self-attention mechanisms along with a decoupled architecture to facilitate OOD generalization in graph learning. However, these approaches fail to account for the essential factors contributing to the performance deterioration of GNNs under diverse distribution shifts. Consequently, their improvements remain limited compared to traditional GNNs. Recent advancements in addressing graph OOD generalization learning have predominantly centered on the core principles of IRM and SCMs, and can be broadly classified into two primary approaches: invariant topolog extraction and invariant spectrum extraction. Specifically, methods such as EERM [29], CIT [31], MARIO [40], CaNet [28] and GRM [27] adopt the first approach by leveraging various mechanisms, including pseudo-environment-generatio, node clustering and contrastive learning, to facilitate the extraction of invariant local topological structures of nodes. Alternatively, SpCo [14] follows the second approach by distinguishing between low-frequency and high-frequency components of the graph spectrum, treating the former as invariant knowledge and the latter as spurious information. This distinction enables the model to enhance OOD generalization through graph contrastive learning. However, as discussed in Section 1, the existence of a universally invariant topology or spectrum is not guaranteed across all graphs in OOD generalization problems. These limitations hinder the performance and generalization capability of existing models, particularly in real-world applications.

3 Methods

3.1 Motivation

As discussed in Section 1, existing graph OOD generalization models exhibit the following limitations: (1) the assumption of an invariant graph topology is not necessarily valid across graphs under different distributions; and (2) the extraction of a universally invariant graph spectrum remains unreliable. These limitations give rise to the following question: what constitutes an appropriate instantiation of invariant knowledge across graphs under multiple distribution shifts?

While existing approaches predominantly rely on either topology or spectrum as the carrier of invariant knowledge, we argue that learnable random walk sequences, sampled according to specific probabilistic rules, provide a more suitable representation of invariant knowledge in graph OOD scenarios. The motivations behind this claim is outlined as follows:

Motivation 1: In contrast to existing approaches where neither topology nor spectrum necessarily remains invariant under various distribution shifts, we posit that invariant knowledge can be instantiated in the form of learnable random walk sequences. This perspective is grounded in the observation that invariant knowledge can be encoded within the probability of transitioning to the next node that shares similar semantic information and possesses invariant features. As long as graphs exhibit common invariant patterns across distribution shifts, this property ensures that random walk sequences can effectively capture and preserve the underlying invariant knowledge.

Motivation 2: Furthermore, random walk sequences maintain a well-defined theoretical relationship with the formulation of graph OOD generalization. Specifically, the probability transition matrix governing these sequences can be learned in accordance with the principles underlying graph OOD generalization, ensuring the adaptability and robustness across various distribution shifts of graphs.

Building upon the prior works [29, 31, 14, 28, 40], the problem of OOD generalization in graphs can be reformulated as an optimization task. Specifically, it involves minimizing the loss of the worst-case performance of the model across multiple graphs within all possible environments. These environments comprise both the invariant knowledge shared among them and the spurious correlations unique to each specific environment. This problem can be formally expressed as follows:

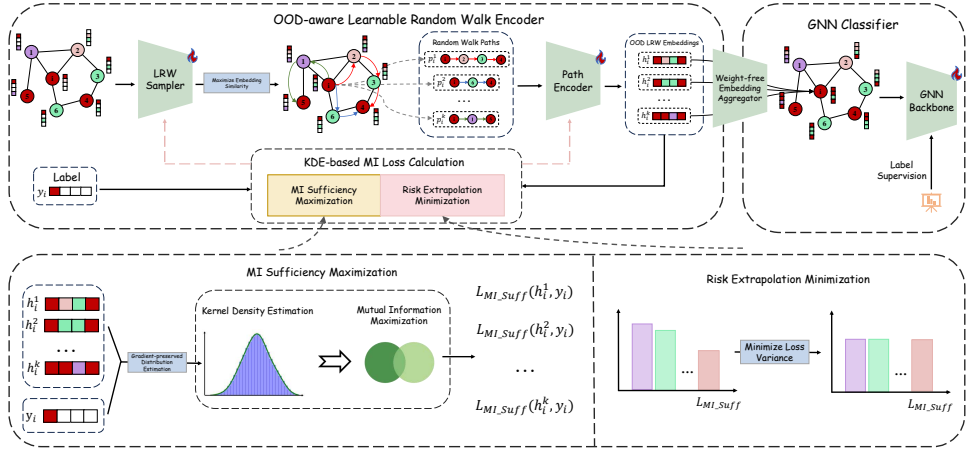


Figure 2: The framework of the proposed LRW-OOD.

$$\min_f \max_{\mathbf{G}_e \sim \mathcal{G}} \mathcal{L}(f(\mathbf{G}_e), \mathbf{y}), \quad (1)$$

where \mathcal{G} is the set of graphs under all environments, \mathbf{G}_e is the graph under the environment e , \mathcal{L} is the loss function, f is the graph OOD model and \mathbf{y} is the label. However, this optimization formulation cannot be directly applied to graph OOD generalization due to the inaccessibility of environmental factors e . To address this challenge, Wu et al. [29] introduces two conditions that are theoretically equivalent to the aforementioned graph OOD generalization formulation while also being directly applicable to graph OOD learning. These conditions are formally stated as follows: (1) sufficient condition: $\mathbf{y} = f^*(\mathbf{G}_e) + \sigma \leftrightarrow \max_f I(\mathbf{y}, f)$, where f^* denotes the model f with the optimal parameters, while σ represents the random variable entirely independent of the predicted label \mathbf{y} . (2) invariance condition: $\Pr(\mathbf{y}|e) = \Pr(\mathbf{y}) \leftrightarrow \min_f I(\mathbf{y}, e|f)$.

It is important to note that random walk sequences can inherently incorporate the two graph OOD generalization conditions by parameterizing the probability transition matrix in accordance with these principles. Specifically, rather than adopting the conventional approach of fixing the probability transition matrix as the degree-normalized adjacency matrix [32, 22], it can instead be parameterized as a learnable matrix. This matrix is initialized using the cosine similarity matrix, which captures the semantic similarity between the soft embeddings of node pairs within graphs, thereby integrating node semantic information into the random walk sequences. However, the semantic similarity matrix alone cannot reliably capture the invariant knowledge across graphs under multiple distribution shifts, as it is susceptible to spurious correlations arising in different environments. To address this limitation, the learnable probability transition matrix must be guided by a distribution-invariant loss that adheres to the two graph OOD generalization conditions outlined above. The details of this approach will be elaborated in the following section.

3.2 Model Framework

The overall framework of the proposed LRW-OOD method is illustrated in Figure 2. Our approach adopts a two-stage training paradigm for OOD generalization in graph learning: (1) the initial stage focuses on training an OOD-aware Learnable Random Walk (LRW) encoder, and (2) the subsequent stage involves training a GNN-based classifier. The LRW encoder is designed to produce high-quality node embeddings that capture invariant features across diverse distribution shifts. These embeddings are then utilized by the GNN classifier—built upon standard GNN backbones such as GCN [9] or GAT [25]—through a weight-free embedding aggregator (i.e., mean-pooling or concatenation) to support various downstream tasks. Given that the primary objective of this paper is to enable graph OOD generalization learning via learnable random walk sequences, the subsequent of the section will primarily focus on the detailed formulation and design of the proposed OOD-aware LRW encoder.

OOD-aware Learnable Random Walk Encoder. To enable the extraction of invariant knowledge from graphs under various distribution shifts, we introduce the OOD-aware Learnable Random Walk (LRW) encoder, depicted in the top-left corner of Figure 2. Departing from conventional random walk strategies—which typically utilize a fixed degree-normalized adjacency matrix as the transition probability matrix [32, 22]—we propose a more adaptive approach. Specifically, the LRW sampler employs a GNN to generate soft node embeddings from the original node features. These embeddings are then used to construct a similarity-based transition matrix, which guides the sampling of k random walk paths. This mechanism enables the integration of both topological and semantic information inherent in the graph data. Formally, for a given node v_i , and given the graph topology \mathbf{A} and node features \mathbf{X} , the LRW sampler generates k random walk paths $\{p_i^r\}_{r=1}^k$ as follows:

$$\{p_i^r\}_{r=1}^k = \text{RW}(v_i, k), \quad \text{s.t. } \Pr_{v_j \in \mathcal{N}(v_i)}(v_i \rightarrow v_j) = \cos(\mathbf{z}_i, \mathbf{z}_j), \quad \mathbf{z} = \text{GNN}(\mathbf{A}, \mathbf{X}), \quad (2)$$

where $\mathcal{N}(v_i)$ denotes the set of neighboring nodes of v_i , and $\text{RW}(v_i, k)$ represents the random walk sampler that generates k random walk paths initiated from node v_i . After obtaining k random walk paths started at node v_i , we then apply a path encoder (i.e., MLP) to transform the embeddings of nodes along the r -th random walk path into the LRW embeddings \mathbf{h}_i^r :

$$\mathbf{h}_i^r = \text{MLP}(\text{Concat}(\{\mathbf{z}_j\}_{v_j \in p_i^r})), \quad \text{s.t. } 1 \leq r \leq k. \quad (3)$$

The resulting LRW embeddings $\{\mathbf{h}_i^r\}_{r=1}^k$, together with the corresponding label \mathbf{y}_i of node v_i , are subsequently input into a kernel density estimation (KDE)-based mutual information (MI) loss module. This component serves as a key component within the LRW encoder, facilitating the model’s ability to capture the invariant knowledge and discard the spurious correlations under OOD scenarios.

KDE-based MI Loss Calculator. As discussed in Section 3.1, the graph OOD generalization can be formulated as an optimization task aimed at minimizing the loss under the worst-case distribution shift. Also, this objective is theoretically equivalent to the two OOD conditions: (1) sufficiency condition, expressed as $\mathbf{y} = f^*(\mathbf{G}_e) + \sigma \leftrightarrow \max_f I(\mathbf{y}, f)$, and (2) invariance condition, given by $\Pr(\mathbf{y}|e) = \Pr(\mathbf{y}) \leftrightarrow \min_f I(\mathbf{y}, e|f)$. To encourage the LRW encoder to generate node embeddings that capture invariant features while discarding spurious correlations, we introduce two complementary objectives: the *MI sufficiency maximization loss* and the *risk extrapolation minimization loss*, which correspond to the sufficiency and invariance conditions, respectively.

To achieve the sufficiency condition, a natural approach would be to directly maximize the mutual information [21, 12] between the LRW embeddings $\{\mathbf{h}_i^r\}_{r=1}^k$ and the corresponding label \mathbf{y}_i . However, this approach is unfeasible due to the agnosticism of the latent label distribution $\Pr(\mathbf{y})$ in the context of graph OOD generalization [28, 40]. As a result, traditional graph OOD models often resort to distance-based loss functions, such as KL divergence, to approximately satisfy the sufficiency condition [29, 27]. Nevertheless, these methods are prone to inaccuracies due to the approximations they involve. In contrast, our proposed MI sufficiency maximization approach leverages an estimation-based mechanism to approximate the distributions of the LRW embeddings $\{\Pr(\mathbf{h}_i^r)\}_{r=1}^k$ and the label distribution $\Pr(\mathbf{y})$, allowing the model to directly compute and maximize the mutual information between these variables. Rather than relying on histogram-based estimation methods—which are non-differentiable due to the discrete partitioning of the hypercubes—we utilize kernel density estimation (KDE) with a Gaussian kernel [15, 21, 12]. This choice is motivated by the differentiability of KDE and its computational efficiency, which allows for gradient-based optimization. The formal expression of this approach is provided below:

$$\mathcal{L}_{\text{MI_Suff}}(\mathbf{h}_i^r, \mathbf{y}_i) = -\hat{\Pr}(\mathbf{h}_i^r, \mathbf{y}_i) \log_2 \frac{\hat{\Pr}(\mathbf{h}_i^r, \mathbf{y}_i)}{\hat{\Pr}(\mathbf{h}_i^r)\hat{\Pr}(\mathbf{y}_i)}, \quad \text{s.t. } \hat{\Pr}(\mathbf{s}) = \frac{e^{-u^2/2}}{(2\pi)^{d/2}m^d \det(\mathbf{S}^{1/2})}, \quad (4)$$

where d represents the dimension of the random variable \mathbf{s} , m denotes the kernel bandwidth, \mathbf{S} is the covariance matrix associated with the random variable \mathbf{s} , and u signifies the variance of \mathbf{s} . Meanwhile, following the prior works [29, 27], we introduce the risk extrapolation minimization loss by minimizing the variance among the MI sufficiency maximization losses $\{\mathcal{L}_{\text{MI_Suff}}(\mathbf{h}_i^r, \mathbf{y}_i)\}_{r=1}^k$. Based on the illustration above, we propose the overall KDE-based MI loss formulated as below:

$$\mathcal{L} = \sum_{i=1}^n \left(\mathbb{V}(\{\mathcal{L}_{\text{MI_Suff}}(\mathbf{h}_i^r, \mathbf{y}_i)\}_{r=1}^k) + \frac{1}{k} \sum_{r=1}^k \mathcal{L}_{\text{MI_Suff}}(\mathbf{h}_i^r, \mathbf{y}_i) \right). \quad (5)$$

3.3 Theoretical Discussion

In this section, we will illustrate the theoretical guarantee that the proposed KDE-based MI loss formulated as equation 5 is capable of guiding a valid random walk sampling for graph OOD generalization formulated as Equation 1. Moreover, we will also give a theoretical upper bound of LRW-OOD, showcasing the computation-friendly property of the proposed model. The detailed proofs for the following theorems are illustrated in the Appendix A.

Theorem 3.1. *Let $f(\mathbf{G}_e)$ denotes the learnable random walk encoder. If it is optimized by minimizing the KDE-based MI loss defined in Equation 5, then the resulting encoder satisfies both the sufficiency condition: $\mathbf{y} = f^*(\mathbf{G}_e) + \sigma$ and the invariance condition: $\Pr(\mathbf{y}|e) = \Pr(\mathbf{y})$.*

Building upon Theorem 3.1, we establish the theoretical guarantee that connects the OOD conditions to the formulation of graph OOD generalization through the following theorem:

Theorem 3.2. *Let $f^*(\mathbf{G}_e)$ denotes the optimized learnable random walk encoder satisfying both the sufficiency and invariance conditions. Then, the encoder $f^*(\mathbf{G}_e)$ is the solution to the graph OOD generalization formulated as Equation 1.*

The preceding theorems establish that the learnable random walk encoder, optimized by the KDE-based MI loss, is theoretically capable of generating random walk sequences that preserve invariant information while effectively eliminating spurious correlations across datasets exhibiting distributional shifts. Furthermore, with the OOD-awareness guaranteed by theorems above, we proceed to demonstrate the model’s time efficiency and memory efficiency through the following theorem:

Theorem 3.3. *Let n, k, s, d be the number of nodes, the times of random walk per node, the walk length per node and the feature dimension, l_1 be the number of layers for the LRW sampler, and l_2 be the number of layers for the path encoder. Then, the overall time complexity and space complexity of LRW-OOD is $\mathcal{O}(nd^2(l_1 + l_2) + nksd)$ and $\mathcal{O}(nd(l_1 + l_2))$, respectively.*

4 Experiments

In this section, we conduct a series of comprehensive experiments to evaluate the performance of the proposed LRW-OOD model in the context of node classification tasks across multiple datasets subjected to various distribution shifts. The objective of these experiments is to address the following research questions: **Q1**: How does the proposed model perform compared to state-of-the-art models on datasets under various distribution shifts? **Q2**: To what extent do the proposed components of LRW-OOD contribute to its OOD generalization capabilities on graph data? **Q3**: How sensitive is the performance of the proposed model to variations in its hyperparameters? **Q4**: What insights can be obtained from visualizing the representations of the proposed model?

4.1 Experiment Setup

Datasets. In line with prior studies, we employ seven node classification datasets that exhibit diverse sizes, characteristics, and types of distribution shifts. These datasets are categorized as follows: (1) synthetic datasets: Cora [34], CiteSeer [34], PubMed [34], and LastFMAsia [18]; (2) cross-domain datasets: Twitch [17] and WebKB [16]; and (3) temporal evolution dataset: ogb-ArXiv [8]. For the synthetic datasets, we augment the original node features with the artificially generated noise of environment-specific spurious correlations, whose dimension d_{spu} varies from 20 to 160. Nodes associated with different spurious environments are then assigned to the training and testing sets, respectively, to simulate distributional shifts. In the case of the cross-domain datasets, we perform a subgraph-level split, such that nodes from distinct domains are separated into the training and testing sets. For the temporal evolution dataset, we conduct a chronological split based on publication year, using papers published before 2017 for training, those published in 2018 for validation and the remaining for testing. A comprehensive summary of the datasets is provided in Table 2, with additional details about data pre-processing presented in Appendix B.

Baselines. We evaluate the performance of the proposed LRW-OOD model against nine state-of-the-art graph OOD generalization methods, namely ERM, IRM, SRGNN, SpCo, EERM, CIT, DGNN, CaNet, and MARIO. To mitigate the effects of randomness and ensure reliable evaluation, each experiment is repeated 10 times, and the average performance is reported. Considering the large number of baseline models, we strategically diversify their inclusion across different experimental

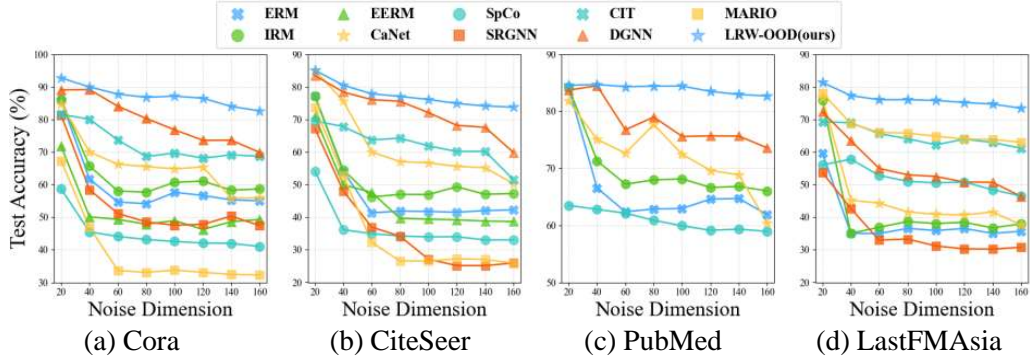


Figure 3: The performance comparison of graph OOD models using GCN as the backbone.

settings. This approach facilitates comprehensive comparisons while avoiding overly complex visualizations, thereby enhancing the clarity and interpretability of the results.

Experiment Environment. To facilitate reproducibility, we report the hardware and software configurations used in our experiments. All experiments were conducted on a server equipped with an Intel(R) Xeon(R) Gold 6240 CPU 2.60GHz, and a NVIDIA A800 GPU with 80GB memory, utilizing CUDA version 12.4. The operating system is Ubuntu 20.04.4 LTS and is configured with 1.0 TB of system memory.

4.2 Performance Comparison

In this Section, we aim to answer **Q1**: How does the proposed LRW-OOD perform compared to state-of-the-art models on datasets under various distribution shifts? To this end, We conduct a comprehensive evaluation of our model against other models across various kinds of datasets, including synthetic datasets, cross-domain datasets and the temporal evolution dataset. The results are shown in Figure 3, Figure 4 and Table 1. Due to the page limit, Figure 4 is put in the Appendix C.

Table 1: The performance of graph OOD models on the corss-domain and temporal evolution datasets.

Dataset	Backbone	ERM	IRM	EERM	SpCo	SRGNN	CIT	CaNet	DGNN	MARIO	LRW-OOD
Twitch	GCN	52.1±1.6	52.1±1.7	OOM	49.0±0.4	47.8±2.4	53.9±0.3	54.3±0.8	52.7±3.1	53.9±0.1	55.5±1.0
	GAT	51.8±1.0	51.5±1.0	OOM	46.9±1.6	53.9±0.1	54.0±0.4	54.0±0.2	53.8±0.2	54.4±0.3	55.3±1.3
WebKB	GCN	9.8±0.1	9.8±0.1	28.4±10.3	9.8±0.1	9.9±0.2	16.0±1.0	11.9±5.7	48.8±12.7	40.4±18.2	52.0±1.9
	GAT	9.9±0.2	10.6±2.0	29.5±18.2	15.3±2.9	56.5±0.9	9.8±0.1	19.5±9.4	37.7±21.9	41.4±17.3	56.7±3.1
ogb-ArXiv	GCN	52.7±0.2	53.1±0.4	39.7±1.4	OOM	48.3±0.5	OOM	52.8±2.0	44.8±0.6	OOM	57.7±0.1
	GAT	52.8±0.2	53.9±0.3	46.7±0.5	OOM	49.2±0.7	OOM	57.1±2.7	43.1±2.1	OOM	58.9±0.1

Distribution Shifts on Synthetic Datasets. We report the testing accuracy on the Cora, CiteSeer, PubMed, and LastFMAsia, each augmented with environment-specific spurious noise features of varying dimensions, ranging from 20 to 160, as illustrated in Figure 3 and Figure 4. While all evaluated models exhibit a decline in performance as the dimensionality of the spurious features increases, the proposed LRW-OOD consistently achieves superior accuracy compared to all baseline methods, regardless of employing GCN or GAT as the backbone. These results highlight the robust graph OOD generalization capability of LRW-OOD in the presence of complex distribution shifts.

Distribution Shifts on Cross-domain & Temporal Evolution Datasets. As presented in Table 1, we report the test accuracy on the WebKB, Twitch, and ogb-ArXiv. The proposed LRW-OOD demonstrates consistently strong performance, significantly outperforming all baseline methods, despite the challenges of substantial domain/temporal distribution shifts within these datasets. Specifically, LRW-OOD achieves an average improvement of approximately 3.1% when using the GCN backbone and around 1.0% with the GAT backbone compared to the sub-optimal baselines. These results underscore the model’s ability to effectively learn invariant representations while mitigating the influence of domain-specific and temporal-specific spurious correlations, thereby highlighting its potential for robust deployment in real-world scenarios.

4.3 Ablation Study

To answer **Q2**, we present a comprehensive ablation analysis of the contribution of each individual component within LRW-OOD across Cora, CiteSeer, PubMed, and LastFMAsia. The experiment results are summarized in Table 3, which is put in Appendix C due to the page limit. Specifically, w/o SM refers to the variant of LRW-OOD where the sufficiency maximization loss is modified by substituting the original KDE-based approach with KL-divergence, following established methodologies in prior literature [29, 27]. w/o REM indicates the model configuration without the risk extrapolation minimization loss. Finally, w/o LRW corresponds to the vanilla random-walk-based GNN model without the proposed LRW encoder. From Table 3, it can be observed that LRW-OOD without the LRW encoder achieves the worst performance compared to that without SM loss and that without REM loss, which emphasizes the great importance of the LRW encoder as the extractor of the invariant knowledge. Meanwhile, we also observe that LRW-OOD without REM loss achieves a better performance compared to that without SM loss on most of the datasets, which demonstrates that the SM loss plays a more important role than the REM loss for the graph OOD generalization.

4.4 Sensitivity Analysis

To answer **Q3**, we investigate the impact of key hyperparameters—specifically, the number of random walk steps and the number of random walk times—on the performance of the proposed LRW-OOD. The evaluation is conducted across multiple datasets, including Cora, CiteSeer, PubMed, and LastFMAsia. The corresponding experimental results are presented in Table 4 and Table 5, which are put in Appendix C due to the page limit. As illustrated in Table 4, LRW-OOD achieves optimal performance with a single-step on the Cora, CiteSeer, and PubMed. In contrast, more walk steps are required to attain the best results on LastFMAsia. This discrepancy can be attributed to differing levels of homophily across datasets: Cora, CiteSeer, and PubMed exhibit more homophily, wherein the invariant knowledge is predominantly localized within the 1-hop neighborhood. Conversely, LastFMAsia demonstrates lower homophily, implying that invariant patterns reside in higher-order neighborhoods. As shown in Table 5, LRW-OOD consistently achieves optimal performance when multiple random walks are initiated per node across all evaluated datasets. This observation suggests that each individual random walk may capture environment-specific spurious correlations. By conducting multiple random walks, LRW-OOD is better equipped to retain invariant patterns while effectively mitigating the influence of spurious correlations across walks.

4.5 Model Visualization

To address **Q4**, we visualize the LRW embeddings derived from different orders of random walk paths on four synthetic datasets: Cora, CiteSeer, PubMed, and LastFMAsia, as shown in Figure 5 which is put in Appendix C due to the page limit. The visualizations reveal that LRW embeddings generated from different walk orders exhibit clear distinctions across all datasets. Notably, these datasets are constructed with varying environment-specific spurious correlations, as described in Section 4.1. Consequently, the model learns to encode distinct representations from random walks, effectively mitigating spurious correlations and capturing invariant information shared across environments with various distribution shifts. This results in a more expressive representation that facilitates the learning of predictive relationships beneficial for graph OOD generalization.

5 Conclusion

In this paper, we introduce LRW-OOD, a novel approach for graph OOD generalization at the node level, which necessitates the model’s ability to handle multiple distribution shifts between the training set and the testing set. Distinct from existing methods that primarily rely on graph topology or spectral properties as the medium for invariant knowledge, our method leverages Learnable Random Walk (LRW) sequences to capture such invariant representations. Rather than utilizing a conventional fixed-probability transition matrix (e.g., the degree-normalized adjacency matrix), our framework employs an LRW-based sampler alongside a path encoder to learn LRW embeddings that parameterize the transition probabilities of the random walk. To ensure the generated random walk sequences conform to the OOD principles, we further propose a KDE-based MI loss, which integrates an MI sufficiency maximization component and a risk extrapolation minimization component. Extensive

experimental evaluations demonstrate the superior performance of LRW-OOD in addressing diverse types of distribution shifts across various graph datasets.

References

- [1] Martin Arjovsky, Léon Bottou, Ishaaan Gulrajani, and David Lopez-Paz. Invariant risk minimization. *arXiv preprint arXiv:1907.02893*, 2019.
- [2] Robert B Ash and Catherine A Doléans-Dade. *Probability and measure theory*. Academic press, 2000.
- [3] Alaa Bessadok, Mohamed Ali Mahjoub, and Islem Rekik. Graph neural networks in network neuroscience. *IEEE Transactions on Pattern Analysis and Machine Intelligence*, 45(5):5833–5848, 2022.
- [4] Bo Chen, Jing Zhang, Xiaokang Zhang, Yuxiao Dong, Jian Song, Peng Zhang, Kaibo Xu, Evgeny Kharlamov, and Jie Tang. Gccad: Graph contrastive learning for anomaly detection. *IEEE Transactions on Knowledge and Data Engineering*, 2022.
- [5] Yongqiang Chen, Yonggang Zhang, Yatao Bian, Han Yang, MA Kaili, Binghui Xie, Tongliang Liu, Bo Han, and James Cheng. Learning causally invariant representations for out-of-distribution generalization on graphs. *Advances in Neural Information Processing Systems*, 35:22131–22148, 2022.
- [6] Kai Guo, Hongzhi Wen, Wei Jin, Yaming Guo, Jiliang Tang, and Yi Chang. Investigating out-of-distribution generalization of gnn: An architecture perspective. In *Proceedings of the 30th ACM SIGKDD Conference on Knowledge Discovery and Data Mining*, pages 932–943, 2024.
- [7] Will Hamilton, Zhitao Ying, and Jure Leskovec. Inductive representation learning on large graphs. *Advances in Neural Information Processing Systems*, NeurIPS, 2017.
- [8] Weihua Hu, Matthias Fey, Marinka Zitnik, Yuxiao Dong, Hongyu Ren, Bowen Liu, Michele Catasta, and Jure Leskovec. Open graph benchmark: Datasets for machine learning on graphs. *Advances in Neural Information Processing Systems*, NeurIPS, 2020.
- [9] Thomas N Kipf and Max Welling. Semi-supervised classification with graph convolutional networks. In *International Conference on Learning Representations*, ICLR, 2017.
- [10] J. Klicpera, A. Bojchevski, and S. Günnemann. Predict then propagate: Graph neural networks meet personalized pagerank. In *International Conference on Learning Representations*, ICLR, 2019.
- [11] Masanori Koyama and Shoichiro Yamaguchi. Out-of-distribution generalization with maximal invariant predictor. 2020.
- [12] Alexander Kraskov, Harald Stögbauer, and Peter Grassberger. Estimating mutual information. *Physical Review E—Statistical, Nonlinear, and Soft Matter Physics*, 69(6):066138, 2004.
- [13] Xunkai Li, Jingyuan Ma, Zhengyu Wu, Daohan Su, Wentao Zhang, Rong-Hua Li, and Guoren Wang. Rethinking node-wise propagation for large-scale graph learning. In *Proceedings of the ACM Web Conference*, WWW, 2024.
- [14] Nian Liu, Xiao Wang, Deyu Bo, Chuan Shi, and Jian Pei. Revisiting graph contrastive learning from the perspective of graph spectrum. *Advances in Neural Information Processing Systems*, 35:2972–2983, 2022.
- [15] Young-Il Moon, Balaji Rajagopalan, and Upmanu Lall. Estimation of mutual information using kernel density estimators. *Physical Review E*, 52(3):2318, 1995.
- [16] Hongbin Pei, Bingzhe Wei, Kevin Chen-Chuan Chang, Yu Lei, and Bo Yang. Geom-gcn: Geometric graph convolutional networks. In *International Conference on Learning Representations*, ICLR, 2020.
- [17] Benedek Rozemberczki, Carl Allen, and Rik Sarkar. Multi-scale attributed node embedding. *Journal of Complex Networks*, 9(2):cnab014, 2021.

[18] Benedek Rozemberczki and Rik Sarkar. Characteristic functions on graphs: Birds of a feather, from statistical descriptors to parametric models. In *Proceedings of the 29th ACM international conference on information & knowledge management*, pages 1325–1334, 2020.

[19] Bernard W Silverman. *Density estimation for statistics and data analysis*. Routledge, 2018.

[20] Zixing Song, Xiangli Yang, Zenglin Xu, and Irwin King. Graph-based semi-supervised learning: A comprehensive review. *IEEE Transactions on Neural Networks and Learning Systems*, 2022.

[21] Ralf Steuer, Jürgen Kurths, Carsten O Daub, Janko Weise, and Joachim Selbig. The mutual information: detecting and evaluating dependencies between variables. *Bioinformatics*, 18(suppl_2):S231–S240, 2002.

[22] Daohan Su, Xunkai Li, Zhenjun Li, Yingping Liao, Rong-Hua Li, and Guoren Wang. Dirw: Path-aware digraph learning for heterophily. *arXiv preprint arXiv:2410.10320*, 2024.

[23] Henan Sun, Xunkai Li, Zhengyu Wu, Daohan Su, Rong-Hua Li, and Guoren Wang. Breaking the entanglement of homophily and heterophily in semi-supervised node classification. *arXiv preprint arXiv:2312.04111*, 2023.

[24] Jianheng Tang, Jiajin Li, Ziqi Gao, and Jia Li. Rethinking graph neural networks for anomaly detection. In *International Conference on Machine Learning, ICML*, 2022.

[25] Petar Veličković, Guillem Cucurull, Arantxa Casanova, Adriana Romero, Pietro Lio, and Yoshua Bengio. Graph attention networks. In *International Conference on Learning Representations, ICLR*, 2018.

[26] Srinivas Virinchi, Anoop Saladi, and Abhirup Mondal. Recommending related products using graph neural networks in directed graphs. In *Joint European Conference on Machine Learning and Knowledge Discovery in Databases*. Springer, 2022.

[27] Song Wang, Zhen Tan, Yaochen Zhu, Chuxu Zhang, and Jundong Li. Generative risk minimization for out-of-distribution generalization on graphs. *arXiv preprint arXiv:2502.07968*, 2025.

[28] Qitian Wu, Fan Nie, Chenxiao Yang, Tianyi Bao, and Junchi Yan. Graph out-of-distribution generalization via causal intervention. In *Proceedings of the ACM Web Conference 2024*, pages 850–860, 2024.

[29] Qitian Wu, Hengrui Zhang, Junchi Yan, and David Wipf. Handling distribution shifts on graphs: An invariance perspective. *arXiv preprint arXiv:2202.02466*, 2022.

[30] Zonghan Wu, Shirui Pan, Fengwen Chen, Guodong Long, Chengqi Zhang, and S Yu Philip. A comprehensive survey on graph neural networks. *IEEE Transactions on Neural Networks and Learning Systems*, 32(1):4–24, 2020.

[31] Donglin Xia, Xiao Wang, Nian Liu, and Chuan Shi. Learning invariant representations of graph neural networks via cluster generalization. *Advances in Neural Information Processing Systems*, 36:45602–45613, 2023.

[32] Chenxuan Xie, Jiajun Zhou, Shengbo Gong, Jiacheng Wan, Jiaxu Qian, Shanqing Yu, Qi Xuan, and Xiaoniu Yang. Pathmlp: Smooth path towards high-order homophily. *arXiv preprint arXiv:2306.13532*, 2023.

[33] Keyulu Xu, Weihua Hu, Jure Leskovec, and Stefanie Jegelka. How powerful are graph neural networks? 2019.

[34] Zhilin Yang, William W. Cohen, and Ruslan Salakhutdinov. Revisiting semi-supervised learning with graph embeddings. In *International Conference on Machine Learning, ICML*, 2016.

[35] Wentao Zhang, Ziqi Yin, Zeang Sheng, Yang Li, Wen Ouyang, Xiaosen Li, Yangyu Tao, Zhi Yang, and Bin Cui. Graph attention multi-layer perceptron. *Proceedings of the ACM SIGKDD Conference on Knowledge Discovery and Data Mining, KDD*, 2022.

- [36] Zhen Zhang, Jiajun Bu, Martin Ester, Jianfeng Zhang, Chengwei Yao, Zhi Yu, and Can Wang. Hierarchical graph pooling with structure learning. *arXiv preprint arXiv:1911.05954*, 2019.
- [37] Xinxiao Zhao, Zhiyong Cheng, Lei Zhu, Jiecai Zheng, and Xueqing Li. Ugrec: modeling directed and undirected relations for recommendation. In *Proceedings of the International ACM SIGIR Conference on Research and Development in Information Retrieval, SIGIR*, 2021.
- [38] Yu Zhou, Haixia Zheng, Xin Huang, Shufeng Hao, Dengao Li, and Jumin Zhao. Graph neural networks: Taxonomy, advances, and trends. *ACM Transactions on Intelligent Systems and TechnoLoGy*, 13(1):1–54, 2022.
- [39] Qi Zhu, Natalia Ponomareva, Jiawei Han, and Bryan Perozzi. Shift-robust gnns: Overcoming the limitations of localized graph training data. *Advances in Neural Information Processing Systems*, 34:27965–27977, 2021.
- [40] Yun Zhu, Haizhou Shi, Zhenshuo Zhang, and Siliang Tang. Mario: Model agnostic recipe for improving ood generalization of graph contrastive learning. In *Proceedings of the ACM Web Conference 2024*, pages 300–311, 2024.

A Theoretical Analysis for Section 3.3

Before proceeding with the proofs of the theorems presented in Section 3.3, we first introduce a useful lemma concerning the theoretical effectiveness of kernel density estimation:

Lemma A.1. *Let $I(\mathbf{x}, \mathbf{y})$ be the real mutual information of the random variables \mathbf{x}, \mathbf{y} , and $\hat{I}(\mathbf{x}, \mathbf{y})$ be the corresponding kernel density estimation as defined in equations 4, then $\hat{I}(\mathbf{x}, \mathbf{y})$ converges in probability to $I(\mathbf{x}, \mathbf{y})$, i.e.:*

$$\hat{I}(\mathbf{x}, \mathbf{y}) \xrightarrow{a.s.} I(\mathbf{x}, \mathbf{y}). \quad (6)$$

Proof. Recall from Section 3.3 that the kernel density function we employ is Gaussian kernel function formulated as: $\hat{Pr}(\mathbf{x}) = \frac{e^{-u^2/2}}{(2\pi)^{d/2} m^d \det(\mathbf{X}^{1/2})}$. According to the propositions of Gaussian kernel function [19, 15], we have:

$$\begin{aligned} \int_{-\infty}^{+\infty} \frac{e^{-u^2/2}}{(2\pi)^{d/2} m^d \det(\mathbf{X}^{1/2})} du &= 1, \\ \int_{-\infty}^{+\infty} u \frac{e^{-u^2/2}}{(2\pi)^{d/2} m^d \det(\mathbf{X}^{1/2})} du &= 0, \\ \int_{-\infty}^{+\infty} u^2 \cdot \frac{e^{-u^2/2}}{(2\pi)^{d/2} m^d \det(\mathbf{X}^{1/2})} du &= 1 < +\infty, \end{aligned} \quad (7)$$

which signify the following facts: (1) the integration of Gaussian kernel function is 1; (2) the bias of Gaussian kernel function is 0; and (3) The variance of Gaussian kernel function is bounded. Thus, according to the theorem of Glivenko–Cantelli [2], we have:

$$\begin{aligned} \sup_{\mathbf{x}, \mathbf{y}} |\hat{Pr}(\mathbf{x}, \mathbf{y}) - Pr(\mathbf{x}, \mathbf{y})| &\xrightarrow{a.s.} 0, \\ \sup_{\mathbf{x}} |\hat{Pr}(\mathbf{x}) - Pr(\mathbf{x})| &\xrightarrow{a.s.} 0, \\ \sup_{\mathbf{y}} |\hat{Pr}(\mathbf{y}) - Pr(\mathbf{y})| &\xrightarrow{a.s.} 0, \end{aligned} \quad (8)$$

which illustrate that the distributions and the joint distribution of random variable \mathbf{x}, \mathbf{y} all converge in probability. Given that the continuous form of mutual information $I(\mathbf{x}, \mathbf{y}) = \int_{\mathbf{x}} \int_{\mathbf{y}} Pr(\mathbf{x}, \mathbf{y}) \log_2 \frac{Pr(\mathbf{x}, \mathbf{y})}{Pr(\mathbf{x})Pr(\mathbf{y})} d\mathbf{x}d\mathbf{y}$ and $\hat{I}(\mathbf{x}, \mathbf{y}) = \int_{\mathbf{x}} \int_{\mathbf{y}} \hat{Pr}(\mathbf{x}, \mathbf{y}) \log_2 \frac{\hat{Pr}(\mathbf{x}, \mathbf{y})}{\hat{Pr}(\mathbf{x})\hat{Pr}(\mathbf{y})} d\mathbf{x}d\mathbf{y}$, the formulations of these two mutual information also converge in probability. Thus, the lemma is proved. \square

A.1 Theoretical Proofs for Theorem 3.1

For the sufficiency condition, we have the following fact that minimizing $\mathcal{L}_{MI_Suff}(\mathbf{h}, \mathbf{y}) = -\hat{Pr}(\mathbf{h}, \mathbf{y}) \log_2 \frac{\hat{Pr}(\mathbf{h}, \mathbf{y})}{\hat{Pr}(\mathbf{h})\hat{Pr}(\mathbf{y})}$ is equivalent to maximizing the discrete form of mutual information $I(\mathbf{h}, \mathbf{y})$, according to lemma A.1. Let \mathbf{h}^* be the optimal parameters that satisfy the sufficiency condition $\mathbf{y} = f^*(\mathbf{G}_e) + \sigma$, and \mathbf{h}' be the parameters that are learned by minimizing $\mathcal{L}_{MI_Suff}(\mathbf{h}, \mathbf{y})$. Suppose $\mathbf{h}^* \neq \mathbf{h}'$. Then, according to the definitions of $\mathbf{h}^*, \mathbf{h}'$ and the propositions of mutual information, we have:

$$\begin{aligned} I(\mathbf{h}^*, \mathbf{y}) &= I(\mathbf{h}^*, f^*(\mathbf{h}^*) + \sigma) \\ &= I(\mathbf{h}^*, f^*(\mathbf{h}^*)), \end{aligned} \quad (9)$$

$$\begin{aligned} I(\mathbf{h}', \mathbf{y}) &= I(\mathbf{h}', f^*(\mathbf{h}^*) + \sigma) \\ &= I(\mathbf{h}', f^*(\mathbf{h}^*)). \end{aligned} \quad (10)$$

Since $\mathbf{h}^* \neq \mathbf{h}'$, it's obvious that $I(\mathbf{h}^*, f^*(\mathbf{h}^*)) \geq I(\mathbf{h}', f^*(\mathbf{h}^*))$. However, \mathbf{h}' is obtained by minimizing $\mathcal{L}_{MI_Suff}(\mathbf{h}, \mathbf{y})$, which suggests that $I(\mathbf{h}^*, f^*(\mathbf{h}^*)) \leq I(\mathbf{h}', f^*(\mathbf{h}^*))$. The contradiction exists due to the false prerequisite of $\mathbf{h}^* \neq \mathbf{h}'$. Thus, $\mathbf{h}^* = \mathbf{h}'$, and the sufficiency condition is satisfied.

According to the invariance condition, we have:

$$\begin{aligned} \Pr(\mathbf{y}|e) = \Pr(\mathbf{y}) &\leftrightarrow \frac{\Pr(\mathbf{y}|e)}{\Pr(\mathbf{y})} = 1 \\ &\leftrightarrow \frac{\Pr(\mathbf{y}, e)}{\Pr(\mathbf{y})\Pr(e)} = 1. \end{aligned} \quad (11)$$

Note that $I(\mathbf{y}, e) = \sum_{\mathbf{y}, e} \Pr(\mathbf{y}, e) \log_2 \frac{\Pr(\mathbf{y}, e)}{\Pr(\mathbf{y})\Pr(e)}$. Thus, given the fact that $I(\mathbf{y}, e) \geq 0$, equation 11 is equivalent to minimizing $I(\mathbf{y}, e)$. According to the chain law of mutual information, $I(\mathbf{y}, e) \leq I(\mathbf{y}, e|\mathbf{h})$. As a consequence, minimizing $I(\mathbf{y}, e|\mathbf{h})$ is equivalent to minimizing $I(\mathbf{y}, e)$. Also, given the definitions of mutual information and KL divergence, we have:

$$\begin{aligned} I(\mathbf{y}, e|\mathbf{h}) &= \text{KL}(\Pr(\mathbf{y}|\mathbf{h}, e) || \Pr(\mathbf{y}|\mathbf{h})) \\ &= \text{KL}(\Pr(\mathbf{y}|\mathbf{h}, e) || \mathbb{E}_e(\mathbf{y}|\mathbf{h}, e)) \\ &\leq \text{KL}(\Pr(\mathbf{y}|\mathbf{h}) || \mathbb{E}_e(\mathbf{y}|\mathbf{h})) \\ &\leq \mathbb{V}_e(\mathbf{y}|\mathbf{h}), \end{aligned} \quad (12)$$

where the first inequality is achieved due to the inaccessibility of the spurious environment e , and the second inequality is achieved due to the convexity of KL divergence and the Jensen Inequality. As the sufficiency condition illustrated above, the predicted label \mathbf{y} is derived from the embedding \mathbf{h} optimized by minimizing $\mathcal{L}_{\text{MI_Suff}}$. Thus, minimizing the risk extrapolation term $\mathbb{V}(\{\mathcal{L}_{\text{MI_Suff}}(\mathbf{h}_i^r, \mathbf{y}_i)\}_{r=1}^k)$ in the equation 5 is capable of minimizing $\mathbb{V}_e(\mathbf{y}|\mathbf{h})$, thus realizing the invariance condition.

A.2 Theoretical Proofs for Theorem 3.2

As illustrated as the equation 1, the OOD formulation requires models to enhance the worst-case performance among multiple graphs within all possible latent environments. Thus, to prove theorem 3.2, we need to prove the value of the KDE-based MI loss $\mathcal{L}(f^*(\mathbf{G}_e), \mathbf{y})$ calculated under the optimal parameters f^* is less than $\mathcal{L}(f(\mathbf{G}_e), \mathbf{y})$ under any sub-optimal parameters f , formulated as:

$$\max_{\mathbf{G}_e \sim \mathcal{G}} \mathcal{L}(f(\mathbf{G}_e), \mathbf{y}) \geq \max_{\mathbf{G}_e \sim \mathcal{G}} \mathcal{L}(f^*(\mathbf{G}_e), \mathbf{y}). \quad (13)$$

The formulation above is equivalent to proving the statement that given any kinds of parameters f , there exists a graph under certain environment $\mathbf{G}'_e \sim \mathcal{G}$ and the corresponding loss value of $\mathcal{L}(f(\mathbf{G}'_e), \mathbf{y})$, such that the loss value of $\mathcal{L}(f^*(\mathbf{G}_e), \mathbf{y})$ under any graph $\mathbf{G}_e \sim \mathcal{G}$ is less than that of $\mathcal{L}(f(\mathbf{G}'_e), \mathbf{y})$, formulated as below:

$$\mathcal{L}(f(\mathbf{G}'_e), \mathbf{y}) \geq \mathcal{L}(f^*(\mathbf{G}_e), \mathbf{y}). \quad (14)$$

Note that the optimized parameter f^* has satisfied the sufficiency condition $\mathbf{y} = f^*(\mathbf{G}_e) + \sigma$, which suggests that the loss of f^* is minimized compared to other kinds of parameters f under the graph \mathbf{G}'_e . We can derive that $\mathcal{L}(f(\mathbf{G}'_e), \mathbf{y}) \geq \mathcal{L}(f^*(\mathbf{G}'_e), \mathbf{y})$. Moreover, the optimized parameter f^* has also satisfied the invariance condition $\Pr(\mathbf{y}|e) = \Pr(\mathbf{y})$, which suggests that the loss of f^* is minimized under any graph with arbitrary environment \mathbf{G}_e . As a result, We can obtain that $\mathcal{L}(f^*(\mathbf{G}'_e), \mathbf{y}) \geq \mathcal{L}(f^*(\mathbf{G}_e), \mathbf{y})$. Based on the illustration above, the theorem 3.2 is thus proved.

A.3 Theoretical Proofs for Theorem 3.3

In this section, we provide a detailed theoretical analysis to establish the computational efficiency of the proposed model, as formalized in Theorem 3.3. Let n denote the number of nodes, k the number of random walks initiated per node, s the length of each walk, and d the dimensionality of node features. Furthermore, let l_1 and l_2 represent the number of layers in the GNN-based LRW sampler and the MLP-based path encoder, respectively. The LRW sampler utilizes a GNN with l_1 layers to compute LRW embeddings, incurring a time complexity of $\mathcal{O}(nd^2l_1)$. Similarly, the path encoder, implemented as an l_2 -layer MLP, introduces an additional time complexity of $\mathcal{O}(nd^2l_2)$. Regarding the learnable random walk process, each node initiates k random walks of length s , and at each step computes cosine similarities between its own LRW embedding and those of its neighbors. This operation results in a time complexity of $\mathcal{O}(nksd)$. Consequently, the total time complexity of the

proposed LRW-OOD model can be expressed as $\mathcal{O}(nd^2(l_1 + l_2) + nksd)$. The space complexity of LRW-OOD is composed of LRW embeddings and the path embeddings generated in the LRW sampler and the path encoder. Thus, the overall space complexity of the proposed model is $\mathcal{O}(nd(l_1 + l_2))$. Thus, Theorem 3.3 is proved.

B Datasets and Pre-processing

In this section, we describe the experimental datasets used in this paper, along with the corresponding data pre-processing procedures and dataset splitting strategies. The datasets are categorized into three distinct groups based on the type of distribution shift they represent: synthetic datasets, cross-domain datasets, and a temporal evolution dataset. These correspond to artificial shifts, cross-domain shifts, and temporal shifts, respectively, as summarized in Table 2. The subsequent subsections provide a detailed account of the pre-processing steps and data partitioning strategies applied to each category.

Table 2: The detailed information of the original datasets.

Distribution shift	Dataset	#Nodes	#Edges	#Features	#Classes	Train/Val/Test
Artificial Shift	Cora	2,708	5,429	1,433	7	Domain-level
	CiteSeer	3,327	4,732	3,703	6	Domain-level
	PubMed	19,717	44,338	500	3	Domain-level
	LastFMAAsia	7,624	55,612	128	18	Domain-level
Cross-domain Shift	Twitch	34,120	892,346	2,545	2	Domain-level
	WebKB	617	1,138	1,703	5	Domain-level
Temporal Shift	ogb-ArXiv	169,343	1,116,243	128	40	Time-level

B.1 Synthetic Datasets Pre-processing

Cora, CiteSeer, PubMed, and LastFMAAsia are four widely utilized benchmark datasets for node classification tasks, frequently employed to evaluate the performance and design of GNNs. The Cora, CiteSeer, and PubMed datasets represent citation networks, where nodes correspond to academic papers and edges denote citation relationships between them. LastFMAAsia is a social network dataset in which nodes represent users of the LastFM platform, and edges indicate friendship relations among users.

For each dataset, we first duplicate the original graph by n_{env} times (the number of latent environments), each one prepared for being augmented by the corresponding spurious environment-sensitive noise. Then, we use the adjacency matrix and the label to construct the spurious noise. Specifically, assume the adjacency matrix as \mathbf{A} , the original node features as \mathbf{X}_{ori} and the node label as \mathbf{y} . Then we adopt a randomly initialized GNN (with the adjacency matrix \mathbf{A} and the node label \mathbf{y}) to generate the invariant node features, denoted as \mathbf{X}_{inv} . Then, we employ another randomly initialized MLP (with input of a Gaussian noise whose mean value is the corresponding environment id within n_{env}) to generate spurious node features \mathbf{X}_{spu} . By integrating the invariant and spurious node features together, we obtain the node features with the artificial distribution shift $\mathbf{X}_{art} = \mathbf{X}_{inv} + \mathbf{X}_{spu}$. After that, we concatenate the original node features and the features with artificial distribution shift $\mathbf{X} = [\mathbf{X}_{ori}, \mathbf{X}_{art}]$ as input node features for training and evaluation. In this way, we construct $n_{env} = 5$ graphs with different environment id's for each dataset. For all baselines, we use three environments for training, one for validation and report the classification accuracy on the remaining graph.

B.2 Cross-domain Datasets Pre-processing

A common scenario in which distribution shifts arise in graph-structured data is cross-domain transfer. In many real-world applications, multiple observed graphs may be available, each originating from a distinct domain. For instance, in the context of social networks, domains can be defined based on the geographic or demographic context in which the networks are collected. More generally, graph data typically captures relational structures among a specific set of entities, and the nature

of interactions or relationships often varies significantly across different groups. As a result, the underlying data-generating distributions differ between domains, giving rise to domain shifts.

The Twitch and WebKB datasets exemplify cross-domain distribution shifts as described above. The Twitch dataset comprises six distinct networks, each representing a different geographical region—specifically, DE, PT, RU, ES, FR, and EN. In these networks, nodes correspond to Twitch users of game streaming, and edges represent friendship relations among them. While these networks share invariant characteristics—such as the majority of users being game streamers—they also exhibit region-specific spurious correlations (e.g., users from a particular region may demonstrate preferences for certain games). This combination of shared and domain-specific features makes Twitch a suitable dataset for evaluating OOD generalization under cross-domain shifts. For all baseline models, we use the networks from DE and PT as the training domains, those from RU and ES for validation, and the remaining networks (FR and EN) for testing.

Another dataset is WebKB which consists of three networks (i.e., Wisconsin, Cornell and Texas) of web pages collected from computer science departments of different universities. In each network, nodes represent web pages and edges represent the hyperlink between them. On the one hand, these networks share some invariant knowledge since they are all collected from the computer science departments; on the other hand, they also contain spurious correlations due to the fact that these departments from different universities may have different research focuses. As a result, these properties make WebKB an ideal OOD dataset with various cross-domain distribution shifts. For all baselines, we employ the network from Wisconsin for the training set, that from Cornell for the validation set and the remaining for the testing set.

B.3 Temporal Evolution Datasets Pre-processing

Another prevalent scenario for OOD generalization arises in the context of temporal graphs, which evolve dynamically over time through the addition or deletion of nodes and edges. As illustrated in Figure 1(a) of Section 1, such graphs are common in large-scale real-world applications, including social and citation networks, where the distributions of node features, topological structures, and labels often exhibit strong temporal dependencies at varying time scales. To investigate temporal distribution shifts in node classification, we employ the widely-used ogb-ArXiv dataset, which provides a benchmark setting for evaluating model performance under temporal dynamics. The ogb-ArXiv dataset consists of 169,343 nodes, each representing a computer science paper from the arXiv repository, with 128-dimensional feature vectors. It contains 1,116,243 edges that capture citation relationships between papers, and 40 distinct node labels corresponding to the subject areas of the papers. This dataset serves as a representative benchmark for OOD generalization under temporal distribution shifts, as citation behaviors naturally evolve over time. For all baseline models, papers published prior to 2017 are used for training, those published in 2018 for validation, and the remaining papers for testing.

C Additional Experimental Results

In this section, we provide the additional experimental results illustrated in Section 4. Figure 4 is the experiment results of the performance comparison from Section 4.2. Table 3 is the experiment results of the ablation study from Section 4.3. Table 4 and Table 5 are the experiment results of the sensitivity study from Section 4.4. Figure 5 is the experiment results of the model visualization from Section 4.5.

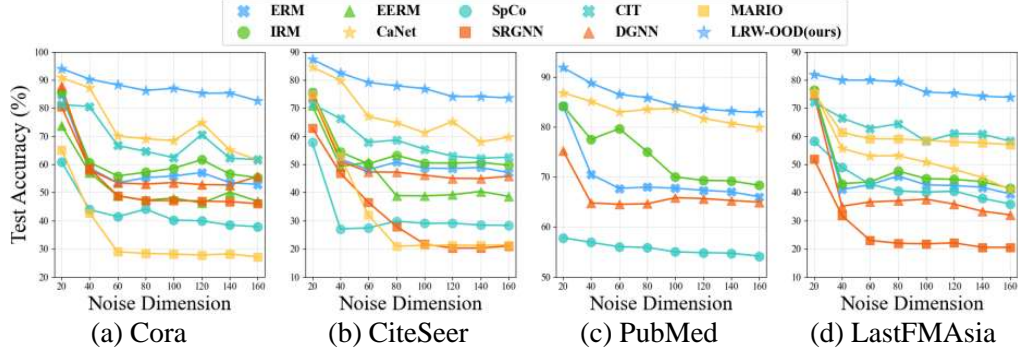


Figure 4: The performance comparison of graph OOD models using GAT as the backbone.

Table 3: The ablation performance for LRW-OOD.

Backbone	Model	Cora	CiteSeer	PubMed	LastFMAsia
GCN	LRW-OOD	82.63±0.64	73.79±1.69	82.71±0.13	73.62±0.45
	w/o SM	81.47±1.01	71.94±0.41	82.13±0.10	71.71±0.45
	w/o REM	81.80±0.57	70.18±0.72	82.16±0.04	73.47±0.34
	w/o LRW	73.4±0.39	59.08±0.27	78.03±0.35	67.4±0.26
GAT	LRW-OOD	82.61±0.03	73.65±0.44	82.84±0.24	73.83±0.78
	w/o SM	81.38±0.84	71.72±0.17	81.86±0.10	72.48±0.87
	w/o REM	81.63±0.58	70.16±0.79	82.07±0.03	73.51±0.6
	w/o LRW	75.1±0.33	59.25±1.03	78.25±0.99	71.79±1.34

Table 4: The performance of LRW-OOD under different hyper-paramenters of random walk steps.

Backbone	Dataset	1-step	2-steps	3-steps	4-steps	5-steps
GCN	Cora	84.4±0.11	83.24±0.14	82.66±0.37	82.63 ±0.64	82.53±0.20
	CiteSeer	74.78±0.64	73.58±0.43	73.25±0.37	73.79±1.69	72.72±0.09
	PubMed	83.14±1.32	82.76±0.78	82.8±0.43	82.71±0.13	82.53±0.54
	LastFMAsia	73.20±0.30	73.32±0.16	73.35±0.23	73.47±0.34	74.36±0.32
GAT	Cora	85.98±0.19	85.01±0.31	84.43±0.43	82.61±0.03	83.75±0.50
	CiteSeer	77.80±0.20	77.06±0.38	76.33±0.54	73.65±0.44	72.98±0.39
	PubMed	83.76±1.48	83.68±0.62	83.12±0.14	82.84±0.24	82.45±0.35
	LastFMAsia	73.44±0.37	73.56±0.06	74.18±0.14	73.83±0.78	72.92±0.15

Table 5: The performance of LRW-OOD under different hyper-paramenters of random walk times.

Backbone	Dataset	1-time	2-times	3-times	4-times	5-times
GCN	Cora	81.52±0.24	82.92±0.13	82.45±0.23	82.63±0.64	83.01±0.23
	CiteSeer	71.54±1.23	72.98±0.29	73.25±0.37	73.79±1.69	73.08±0.24
	PubMed	81.94±0.41	81.88±1.01	82.03±0.14	82.71±0.13	83.01±0.48
	LastFMAsia	71.90±0.54	72.59±0.2	72.43±0.20	73.47±0.34	73.96±0.13
GAT	Cora	81.90±0.43	82.93±0.52	81.49±0.28	82.61±0.03	83.62±0.43
	CiteSeer	72.94±0.67	73.12±0.35	73.33±0.54	73.65±0.44	73.22±0.42
	PubMed	81.96±0.94	82.08±1.14	82.53±0.89	82.84±0.24	83.01±0.84
	LastFMAsia	72.81±0.45	73.00±0.37	73.07±0.11	73.83±0.78	73.98±0.23

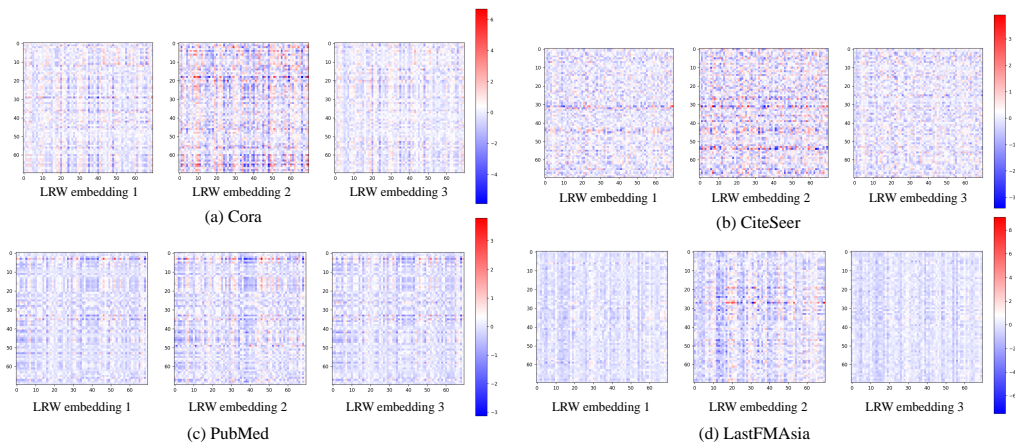


Figure 5: The visualization of weights of LRW-OOD on the synthetic datasets.